JACS
JOURNAL OF THE AMERICAN CHEMICAL SOCIETY

COMMUNICATION

pubs.acs.org/JACS

Light-Induced Enantiospecific 4π Ring Closure of Axially Chiral 2-Pyridones: Enthalpic and Entropic Effects Promoted by H-Bonding

Elango Kumarasamy, Josepha L. Jesuraj, Joseph N. Omlid, Angel Ugrinov, and Jayaraman Sivaguru*

Department of Chemistry and Biochemistry, North Dakota State University, Fargo, North Dakota 58108, United States

Supporting Information

ABSTRACT: Nonbiaryl axially chiral 2-pyridones were synthesized and employed for light-induced electrocyclic 4π ring closure leading to bicyclo-β-lactam photoproducts in solution. The enantioselectivity in the photoproducts varied from 22 to 95% depending on the reaction temperature and the ability of the axially chiral chromophore to form intramolecular and/or intermolecular H-bonds with the solvent. On the basis of the differential activation parameters, entropic control of the enantiospecificity was observed for 2-pyridones lacking the ability to form H-bonds. Conversely, enthalpy played a significant role for 2-pyridones having the ability to form H-bonds.

The role of H-bonds in orchestrating chemical and biological processes in nature defies imagination. Chemists have cleverly taken advantage of H-bonding to perform asymmetric catalytic chemical transformations.[1] While established methodologies for asymmetric thermal reactions exist,[1] light-induced asymmetric reactions[2] in solution have not met the same level of success as their thermal counterparts. Various groups over the last three decades have employed constrained media to achieve stereoselectivity with varying degrees of success.[3] However, achieving stereoselectivity during photoreactions in solution has not been generalized because of the short lifetime of the photoexcited chromophores, which limits the interaction necessary to achieve stereoselectivity. In this regard, we have been exploring the use of nonbiaryl axially chiral chromophores[4,5] to achieve stereoselectivity during photoreactions in solution and have successfully achieved very high enantioselectivity (>90% ee in the photoproduct) in 6π photocyclization and Norrish–Yang reactions.[6] In the present work, a novel class of axially chiral 2-pyridones **1**, where H-bonding contributes to the axial chirality, have been synthesized and employed for light-induced electrocyclic 4π ring closure leading to bicyclo-β-lactam photoproducts, namely, 2-(aryl)-2-azabicyclo[2.2.0]hex-5-en-3-ones (**2**), with very high enantiomeric excess (ee values) in solution.

The photoreactivity of 2-pyridones has been studied in depth in both solution[7a−c] and the solid state.[7d] Depending on the concentration, 2-pyridones can either undergo 4π ring closure or [4+4] photocycloaddition.[7b] The molecularly chiral 2-pyridones **1a**−**c** were synthesized to evaluate the influence of intra- and intermolecular H-bonding[8] on the rotation about the N−C(aryl) chiral axis and to elucidate the transfer of axial chirality to point chirality through weak interactions during photochemical 4π ring closure leading to bicyclo-β-lactams **2** (Scheme 1).

Scheme 1. Light-Induced 4π Ring Closure of 2-Pyridones

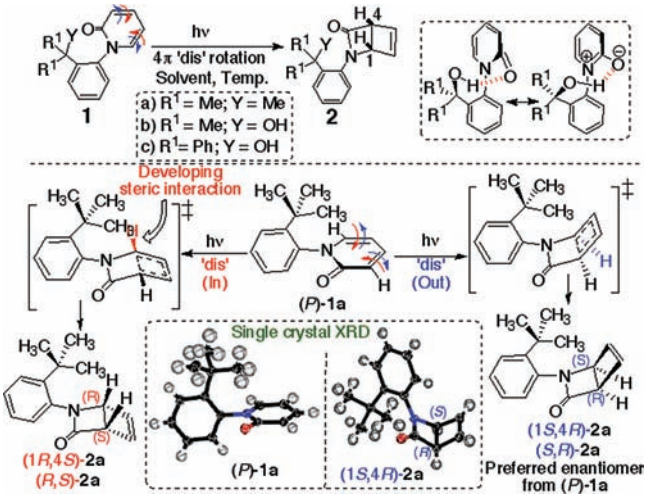

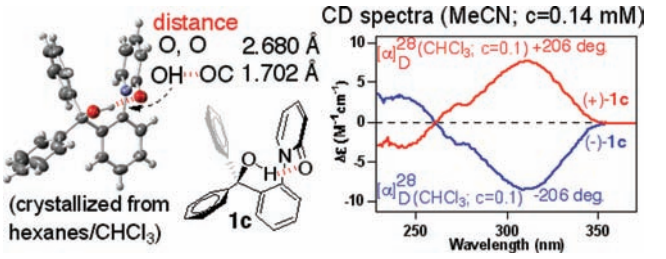

Figure 1. X-ray crystal structure, CD spectra, and $[\alpha]_D$ values of **1c**.

The individual *P* and *M* isomers[9] of **1a**−**c** were easily isolable by HPLC on a chiral stationary phase and characterized by NMR spectroscopy, circular dichroism (CD) spectroscopy, optical rotation, high-resolution mass spectrometry (HRMS), and single-crystal X-ray diffraction (XRD) (Figure 1 and Scheme 1).[10] Analysis of the single-crystal X-ray structure[10] of **1a** revealed that the pyridone ring is perpendicular to the *N*-aryl substituent, possibly reflecting a minimized steric interaction between the pyridone ring and the *o*-*tert*-butyl substituent.[5] Similarly, the single-crystal X-ray structure of **1c** revealed an analogous geometry (Figure 1) in which the pyridone ring is perpendicular to the *N*-aryl substituent. In addition, intramolecular H-bonding between the pyridone amide carbonyl and the 3° hydroxyl

Received: April 4, 2011
Published: October 07, 2011

Table 1. Half-Lives of Racemization ($t_{1/2\text{-rac}}$) for 1 and Values of Enantiomeric Excess for 2 in Various Solvents at Different Temperatures, and the Corresponding Eyring Parameters[a]

Entry	Parameters	$t_{1/2\text{-rac}}$ (days) of 1 [b]				t	Enantiomeric excess (% ee), 2 [f,n]							
		Toluene	CH_3CN	CH_3OH	H_2O		Toluene		MeCN		MeOH		H_2O	
			1a				(*P*)-**1a**	(*M*)-**1a**	(*P*)-**1a**	(*M*)-**1a**	(*P*)-**1a**	(*M*)-**1a**	(*P*)-**1a**	(*M*)-**1a**
1.	T = 65 °C	1.45	5.3	23.5	-[c]	2 h	72 (*S*,*R*)	72 (*R*,*S*)	84 (*S*,*R*)	84 (*R*,*S*)	86 (*S*,*R*)	86 (*R*,*S*)	-[c]	-[c]
2.	T = 45 °C	22.7	77.8	-[d]	-[c]	3 h	76 (*S*,*R*)	76 (*R*,*S*)	82 (*S*,*R*)	82 (*R*,*S*)	88 (*S*,*R*)	88 (*R*,*S*)	-[c]	-[c]
3.	T = 25 °C [g,h]	120	-[d]	-[d]	-[c]	5 h	70 (*S*,*R*)	70 (*R*,*S*)	86 (*S*,*R*)	86 (*R*,*S*)	84 (*S*,*R*)	84 (*R*,*S*)	-[c]	-[c]
4.	T = 5 °C					10 h	72 (*S*,*R*)	72 (*R*,*S*)	88 (*S*,*R*)	88 (*R*,*S*)	82 (*S*,*R*)	82 (*R*,*S*)	-[c]	-[c]
5.	T = -25 °C					15 h	72 (*S*,*R*)	72 (*R*,*S*)	82 (*S*,*R*)	82 (*R*,*S*)	86 (*S*,*R*)	86 (*R*,*S*)	-[c]	-[c]
6.	$\Delta\Delta H^{\ddagger}$ (kcal·mol^{-1})						0.123	-0.123	-0.008	0.008	0.243	-0.243		
7.	$\Delta\Delta S^{\ddagger}$ (cal·K^{-1}·mol^{-1})						4.08	-4.08	4.91	-4.91	5.87	-5.87		
8	% conv [i]						67		74		76		-[c]	
			1b				(+)-**1b**	(-)-**1b**	(+)-**1b**	(-)-**1b**	(+)-**1b**	(-)-**1b**	(+)-**1b**	(-)-**1b**
9.	T = 65 °C [j]	0.6 (h)[e]	1.1 (h)[e]	2.8 (h)[e]	2.5	2 h	21 (B)	22 (A)	51 (B)	51 (A)	62 (B)	61 (A)	93 (B)	93 (A)
10.	T = 45 °C	3.4 (h)[e]	10.6 (h)[e]	21.8 (h)[e]	27.7	3 h	60 (B)	61 (A)	84 (B)	83 (A)	85 (B)	87 (A)	94 (B)	94 (A)
11.	T = 25 °C	1.8	4.6	4.0	-[d]	5 h	64 (B)	65 (A)	76 (B)	77 (A)	87 (B)	88 (A)	93 (B)	93 (A)
12.	T = 5 °C	108	330	-[d]	-[d]	10 h	82 (B)	83 (A)	82 (B)	84 (A)	88 (B)	89 (A)	95 (B)	95 (A)
13.	T = -25 °C					15 h	82 (B)	84 (A)	89 (B)	88 (A)	93 (B)	93 (A)	-[m]	-[m]
14.	$\Delta\Delta H^{\ddagger}$ (kcal·mol^{-1})						-3.519	3.320	-2.386	2.445	-2.843	2.843	-0.847	0.847
15.	$\Delta\Delta S^{\ddagger}$ (cal·K^{-1}·mol^{-1})						-8.82	8.12	-3.88	4.06	-4.55	4.59	4.09	-4.09
16.	% conv [i]						75		87		97		98	
			1c				(-)-**1c**	(+)-**1c**	(-)-**1c**	(+)-**1c**	(-)-**1c**	(+)-**1c**	(-)-**1c**	(+)-**1c**
17.	T = 65 °C [j,k]	0.5 (h)[e]	0.5 (h)[e]	0.3 (h)[e]	-[c]	20 min	69 (B)	69 (A)	70 (B)	70 (A)	86 (B)	86 (A)	-[c]	-[c]
18.	T = 45 °C [k]	1.8 (h)[e]	2.1 (h)[e]	1.3 (h)[e]	-[c]	25 min	88 (B)	88 (A)	90 (B)	90 (A)	90 (B)	90 (A)	-[c]	-[c]
19.	T = 25 °C [k]	46 (h)[e]	46 (h)[e]	15 (h)[e]	-[c]	35 min	94 (B)	94 (A)	94 (B)	94 (A)	97 (B)	97 (A)	-[c]	-[c]
20.	T = 25 °C					2 h	63 (B)	63 (A)	75 (B)	76 (A)	79 (B)	79 (A)	-[c]	-[c]
22.	$\Delta\Delta H^{\ddagger}$ (kcal·mol^{-1})						-8.87	8.87	-8.64	8.64	-8.08	8.08		
23.	$\Delta\Delta S^{\ddagger}$ (cal·K^{-1}·mol^{-1})						-22.7	22.7	-21.8	21.8	-19.0	19.0		
24.	% conv [i,l]						5 (36)		7 (44)		10 (60)		-[c]	

[a] Racemization values (error ±5%) and ee values (average of three trials; ±3% error) were determined by HPLC using a chiral stationary phase. [b] See the Supporting Information (SI) for values of $\Delta G^{\ddagger}_{rac}$ and k_{rac}. [c] Not water-soluble. [d] No observable racemization after 2 months. [e] Values of $t_{1/2\text{-rac}}$ in hours. [f] The signs of optical rotation of **1** in MeOH. For **2a**, (*S*,*R*) and (*R*,*S*) represent the (1*S*,4*R*) and (1*R*,4*S*) configurations, respectively. For **2b** and **2c**, A and B refer to the elution order for a given pair of enantiomers. [g] Similar selectivities were found using Pyrex and 340 nm cutoff filters. [h] The ee values at 25 °C in toluene were 82% (2 h), 76% (4 h), 70% (5 h), and 68% (6 h). Even though there was no noticeable racemization of **1a** in the dark, slow racemization of **1a** was observed in irradiated samples (see the SI). [i] Calculated by ^{1}H NMR spectroscopy with Ph_3CH as an internal standard at 25 °C for 18 h of irradiation. For **1c**, values are given in parentheses. Mass balance was 83−98% depending on the solvent. [j] Noticeable racemization of 2-pyridones **1b** and **1c** occurred at 65 °C (see the SI). [k] For **1c**, $\Delta\Delta H^{\ddagger}$ and $\Delta\Delta S^{\ddagger}$ values were computed at <10% conversion. In MeOH, irradiation times were 5 min (65 °C), 11 min (45 °C), and 12 min (25 °C) to keep the conversion below 10% (see the SI). [l] To ascertain low conversions at 25 °C, irradiation times were 35 min (toluene and MeCN) and 12 min (MeOH). [m] Below the freezing point of the solvent. [n] In the case of **1a**, positive and negative $\Delta\Delta G^{\ddagger}_{SR-RS}$ favor the (1*R*,4*S*)-**2a** and (1*S*,4*R*)-**2a** photoproducts, respectively.

group with a bond length of 1.702 Å was observed. The distance between the two oxygen atoms was 2.68 Å for **1c**, indicating a moderate intramolecular H-bond strength[11] (Figure 1).

To ascertain the role of H-bonding in influencing the axial chirality in **1**, the racemization kinetics of **1a**−**c** was studied in different solvents at various temperatures to establish the half-life ($t_{1/2\text{-rac}}$), rate constant (k_{rac}), and activation free energy ($\Delta G^{\ddagger}_{rac}$) of racemization.[10] For a given solvent at a particular temperature, the racemization rates were ordered as **1c** > **1b** > **1a** (Table 1).[10] Inspection of Table 1 reveals that *o*-*tert*-butyl-substituted 2-pyridone **1a** (which lacks the ability to form an intramolecular H-bond) racemized slowly in comparison with 2-pyridones **1b** and **1c** (which have the ability to form intramolecular H-bonds). For **1b**, polar solvents with the ability to form H-bonds decreased the rate of racemization, as reflected in the higher $t_{1/2\text{-rac}}$ values. For example, at 45 °C, the $t_{1/2\text{-rac}}$ value of **1b** was 3.4 h ($\Delta G^{\ddagger}_{rac}$ = 24.83 kcal mol^{-1}, k_{rac} = 5.6 × 10^{-5} s^{-1}) in toluene, compared with ∼28 days ($\Delta G^{\ddagger}_{rac}$ = 28.17 kcal mol^{-1}, k_{rac} = 2.9 × 10^{-7} s^{-1}) in water (Table 1, entry 10). We believe that the slow racemization of **1b** in polar solvents is likely due to (a) the possibility of resonance-induced H-bonding via the zwitterionic structure[11,12] that might be preferred in polar solvents (Scheme 1, top-right inset) and (b) additional intermolecular H-bonding from polar solvents that form a solvent cluster hindering N−C(aryl) bond rotation.[10,13] This is reflected in the slow N−C(aryl) bond rotation, resulting in higher $t_{1/2\text{-rac}}$ values for **1b** in polar solvents (Table 1). Hence, for **1b**, enantiospecific chiral transfer from polar solvents is expected to be more efficient than from nonpolar solvents. For **1c**, fast racemization with similar k_{rac} values was observed in the solvents investigated. We believe that the hydrophobic phenyl group likely hinders the formation of H-bonding solvent clusters in **1c**, which is reflected in its high racemization rates (Table 1).[10]

Photoirradiation of optically pure atropisomers (*P* or *M*) of **1** was performed using a 450 W medium-pressure Hg lamp with a Pyrex cutoff filter and a cooling jacket under a constant flow of N_2 at various temperatures (−25 to 65 °C) in different solvents (toluene, MeCN, MeOH, and H_2O). The reaction progress and conversion were followed by ^{1}H NMR and/or UV−vis spectroscopy.[10] The reaction was found to be clean and efficient.[10] The conversion was dependent on the temperature, solvent, and irradiation time.[10] For example, **1b** at 25 °C with 18 h of irradiation gave 98% conversion with 91% mass balance in water and 75% conversion with 92% mass balance in toluene (Table 1).[10] The photoproduct **2** was purified by chromatography and characterized by NMR spectroscopy and single-crystal XRD; it was found to be enantiomeric, as ascertained by optical rotation values and CD spectroscopy.[10] It is well-established[14]

dx.doi.org/10.1021/ja203087a |*J. Am. Chem. Soc.* 2011, 133, 17106–17109

that the N−C(aryl) bond with an *o-tert*-butyl substituent can rotate freely because of the reduced C−N−C bond angle in β-lactams. Single-crystal XRD analysis of **2c** revealed an intramolecular H-bonding distance of 1.911 Å, a distance of 2.73 Å between the two oxygen atoms, and a reduced C−N−C bond angle in the β-lactam ring.[10] Similarly, single-crystal XRD analysis of **2a** revealed a reduced C−N−C bond angle in the β-lactam ring.[10]

Table 1 reveals moderate to high enantiomeric excess (ee) in photoproduct **2**. Distinct trends were observed for **1b** and **1c** with the ability to form an intramolecular H-bond and *o-tert*-butyl-substituted **1a** that lacks the ability to form an intramolecular H-bond. For **1a**, there was no observable temperature effect irrespective of the solvent employed (Table 1).[10] For example, for **1a** in MeOH, an ee value of 86% was observed at both 65 and −25 °C. There was minimal variation in the ee values upon changing the solvent from toluene (72%) to methanol (86%). On the other hand, for **1b** and **1c**, the ee values were not only dependent on the solvent but also on the reaction temperature. For example, for **1b**, the ee values at a given temperature were higher in polar solvents with the ability to form H-bonds (water) and progressively decreased with decreasing solvent polarity. The ee values were lower in nonpolar solvents that lacked the ability to form H-bonds (toluene) than in solvents with higher polarity. For example, for **1b** at 65 °C, the ee values in H_2O, MeOH, MeCN, and toluene were 93, 61, 51, and 22%, respectively (Table 1). Similar selectivities were observed with both Pyrex and 340 nm cutoff filters.[10] As 4π ring closure of 2-pyridones is reversible depending on the irradiation wavelength,[7] control studies were carried out by irradiating photoproduct **2a** using both a Pyrex cutoff filter and a >340 nm cutoff filter.[10] As expected, no photoreversion from **2** to **1** was observed, as **2** does not have absorbance beyond 280 nm.[10] The stereochemical course of the photoreaction was deciphered by single-crystal XRD,[10] which showed that (*P*)-**1a** gave (1*S*,4*R*)-**2a** and (*M*)-**1a** gave the optical antipode, (1*R*,4*S*)-**2a**, indicating a well-behaved system. Mechanistically, the 4π dis-"in" rotation was likely hindered by the developing steric interactions, while the 4π dis-"out" rotation was favored, resulting in the observed enantioenriched photoproduct (Scheme 1). Our results raise critical questions pertaining to the temperature and solvent dependence of the ee values during photochemical 4π ring for closure of **1**: What is the role of intra- and intermolecular H-bonding? What is the role of entropic factors and/or enthalpic factors? To address these questions, the differential activation parameters ($\Delta\Delta H^{\ddagger}$ and $\Delta\Delta S^{\ddagger}$) were computed using Eyring plots (eqs 1−3). Because of the fast racemization of **1c** at elevated temperatures (65 °C), we computed $\Delta\Delta H^{\ddagger}$ and $\Delta\Delta S^{\ddagger}$ at low conversions (5−10%) to ascertain their true magnitudes. The ee value given by the $\ln(k_{SR}/k_{RS})$ term is related to $\Delta\Delta G^{\ddagger}$, which depends on both $\Delta\Delta H^{\ddagger}$ and $\Delta\Delta S^{\ddagger}$. The magnitudes and signs of $\Delta\Delta H^{\ddagger}$ and $\Delta\Delta S^{\ddagger}$ help explain the effect of solvent and temperature on ee values in **2**.

$$\ln(k_{SR}/k_{RS}) = \ln[(100 + \%ee)/(100 - \%ee)] \quad (1)$$

$$\ln(k_{SR}/k_{RS}) = \Delta\Delta S^{\ddagger}_{SR-RS}/R - \Delta\Delta H^{\ddagger}_{SR-RS}/RT \quad (2)$$

$$\Delta\Delta G^{\ddagger}_{SR-RS} = \Delta\Delta H^{\ddagger}_{SR-RS} - T\Delta\Delta S^{\ddagger}_{SR-RS} \quad (3)$$

Table 1 reveals that for **1a**, $\Delta\Delta S^{\ddagger}$ is dominant with a near-zero/minimal contribution from $\Delta\Delta H^{\ddagger}$. This is reflected in the Eyring plots, which have near-zero slopes in all the solvents

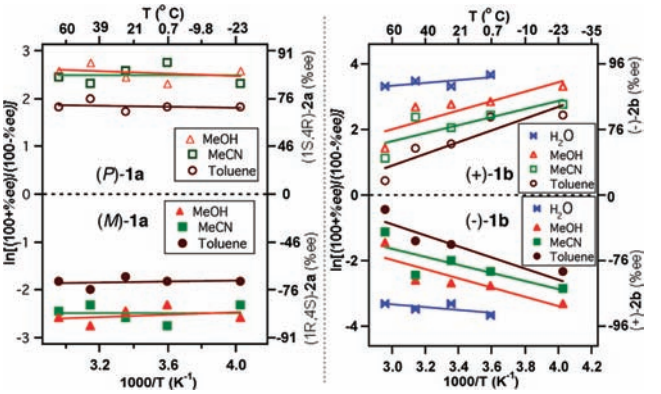

Figure 2. Eyring plot for the photoreactivity of (left) **1a** and (right) **1b**.

investigated (Figure 2 left). Because of the near-zero/minimal contribution from $\Delta\Delta H^{\ddagger}$, the $\ln(k_{SR}/k_{RS})$ term (eq 2) hence the ee values (eq 1) are unaffected by changes in temperature. Thus, for (*P*)-**1a** (Table 1, entries 6 and 7) the positive $\Delta\Delta S^{\ddagger}_{SR-RS}$ value gives $k_{SR} > k_{RS}$, resulting in (1*S*,4*R*)-**2a**. For (*M*)-**1a**, the negative $\Delta\Delta S^{\ddagger}_{SR-RS}$ value gives $k_{SR} < k_{RS}$, leading to the optical antipode (1*R*,4*S*)-**2a**, as observed. Based on the differential activation parameters, we believe that the 4π photocyclization in *o-tert*-butyl-substituted pyridone **1a** is entropically controlled. This speculation is based on the observed free N−C(aryl) bond rotation in the photoproduct **2a** compared with the restricted N−C(aryl) bond rotation in 2-pyridone **1a**.[10] This free N−C(aryl) bond rotation possibly manifests itself in the transition state as entropic control of enantiospecificity, reflecting a higher contribution from $\Delta\Delta S^{\ddagger}$ and minimal contribution from $\Delta\Delta H^{\ddagger}$. For **1b**, the relative contributions from $\Delta\Delta H^{\ddagger}$ and $\Delta\Delta S^{\ddagger}$ depend on the solvent. As the solvent polarity decreases (from water to toluene), the contribution from $\Delta\Delta H^{\ddagger}$ increases (Table 1, entries 14 and 15). There is a substantial contribution from $\Delta\Delta H^{\ddagger}$ in toluene. This higher contribution from $\Delta\Delta H^{\ddagger}$ is reflected in the larger slope values in the Eyring plots (Figure 2 right). The higher values of $\Delta\Delta H^{\ddagger}$ reflect the transition state being influenced by the intramolecular H-bond during the photochemical transformation in toluene (where only an intramolecular H-bond is expected). Apart from the magnitudes of $\Delta\Delta H^{\ddagger}$ and $\Delta\Delta S^{\ddagger}$ in **1b**, it is important to note the sign of $\Delta\Delta H^{\ddagger}$ and $\Delta\Delta S^{\ddagger}$ for a given solvent. In MeOH, MeCN, and toluene, $\Delta\Delta H^{\ddagger}$ and $\Delta\Delta S^{\ddagger}$ have the same sign, while in water, $\Delta\Delta H^{\ddagger}$ and $\Delta\Delta S^{\ddagger}$ have opposite signs. The ee value, which is given by the $\ln(k_{SR}/k_{RS})$ term (eq 1), is thus determined by the relative contributions from $\Delta\Delta H^{\ddagger}$ and $\Delta\Delta S^{\ddagger}$ (eq 2). Additionally, the $\ln(k_{SR}/k_{RS})$ term is influenced by temperature through $\Delta\Delta H^{\ddagger}/RT$ term in eq 2. For **1b**, the $\Delta\Delta H^{\ddagger}$ values are comparable to the $\Delta\Delta S^{\ddagger}$ values in toluene, MeOH, and MeCN. As both $\Delta\Delta H^{\ddagger}$ and $\Delta\Delta S^{\ddagger}$ have the same sign in MeOH, MeCN, and toluene, when the temperature increases, the relative contribution from the $\Delta\Delta H^{\ddagger}/RT$ term decreases, changing the magnitude of the $\ln(k_{SR}/k_{RS})$ term (eq 2). This is reflected in the temperature dependence of the ee values. The change in the magnitude of the $\ln(k_{SR}/k_{RS})$ term (and thus the ee values) is pronounced in toluene, as there is significant contribution from $\Delta\Delta H^{\ddagger}$. Conversely, in water, the contribution from $\Delta\Delta H^{\ddagger}$ is minimal, with a higher contribution from $\Delta\Delta S^{\ddagger}$. As $\Delta\Delta H^{\ddagger}$ and $\Delta\Delta S^{\ddagger}$ carry opposite signs, irrespective of their relative contributions, the magnitude of $\ln(k_{SR}/k_{RS})$ increases, albeit moderately, with

decreasing temperature because of the minimal contribution from the $\Delta\Delta H^{\ddagger}/RT$ term (eq 2). Thus, in water, as $\Delta\Delta H^{\ddagger}$ and $\Delta\Delta S^{\ddagger}$ carry opposite signs for a given axially chiral **1b** (*P* or *M*), the same enantiomer is enhanced with minimal change in the ee value at different temperatures.

For **1c**, a trend similar to that for **1b** was observed in toluene, MeOH and MeCN (Table 1, entries 17−19) . Because of the fast racemization of **1c** at elevated temperatures, $\Delta\Delta H^{\ddagger}$ and $\Delta\Delta S^{\ddagger}$ values were computed at low conversions (5−10%) to gauge their influence in the initial stages of the reaction. Similar to **1b**, the $\Delta\Delta H^{\ddagger}$ values for **1c** are comparable to the $\Delta\Delta S^{\ddagger}$ values for a given reaction temperature in toluene, MeOH, and MeCN. As both $\Delta\Delta H^{\ddagger}$ and $\Delta\Delta S^{\ddagger}$ have the same sign in MeOH, MeCN, and toluene, when the temperature is increased, the relative contribution from the $\Delta\Delta H^{\ddagger}/RT$ term decreases, changing the magnitude of the $\ln(k_{SR}/k_{RS})$ term (eq 2), which is reflected in the temperature dependence of the ee values (similar to **1b**).

The enthalpy−entropy compensation plot[10] gave a straight line passing through the origin, indicating that the same mechanism is operating irrespective of the solvent employed.[15] To comprehend the dichotomy between the solvent and temperature dependences for **1a** versus **1b** and **1c**, it is critical to appreciate the influence of the solvent molecules surrounding the substrates and their influence on both $\Delta\Delta H^{\ddagger}$ and $\Delta\Delta S^{\ddagger}$. For **1a**, few solvent molecules around the amide group will likely be enough to freeze the C−N bond rotation irrespective of the temperature. Hence, the ee values are not affected drastically by changes in the temperature or solvent. Conversely, for **1b** and **1c**, a cluster of intermolecular H-bonds with the solvent in addition to the intramolecular H-bond facilitated by the amide carbonyl and the 3° hydroxyl groups likely contributes to both the differential activation enthalpy and entropy.[10] Temperature plays a crucial role in determining the strength and magnitude of the H-bonds. This dependence is reflected in the solvent and temperature effect on the ee values for **1b** and **1c**.

Qualitatively, the difference in $\Delta\Delta G^{\ddagger}$ [which is related to $\ln(k_{SR}/k_{RS})$] for dis-"in" versus dis-"out" rotations depends not only on the steric impediments but also on the strength and number of H-bonds, which in turn would be dictated by the solvent clusters above and below the plane of the pyridone ring. From Scheme 1, in the *P* isomer, the dis-"in" rotation would have more molecular constraints (steric constraints for **1a**; sterics, H-bonding, and solvent clusters for **1b** and **1c**) than the dis-"out" mode, which is reflected in the $\Delta\Delta G^{\ddagger}$ values. The magnitude of $\Delta\Delta G^{\ddagger}$ is primarily influenced by the entropic difference in the transition state ($\Delta\Delta S^{\ddagger}$) in **1a** for the dis-"in" versus dis-"out" mode of rotation. Conversely for **1b** and **1c**, the magnitude of $\Delta\Delta G^{\ddagger}$ is influenced by both entropic and enthalpic factors dictated by H-bonding.

Our analysis of the Eyring parameters has provided insights into the role of H-bonding and the impact of entropic and enthalpic factors during enantiospecific 4π photocyclization of axially chiral 2-pyridones **1**. The presence of the H-bond(s) (intramolecular and/or intermolecular from the solvent) influences the axial chirality, which is reflected in the half-life of racemization, which is in turn revealed in the enantiospecific chiral transfer. The difference in the diastereomeric transition-state energies for 4π dis-"in" versus 4π dis-"out" ring closure is likely impacted by steric impediments for non-H-bonding substrates (entropic factors), while for substrates that have the ability to form H-bonds, both enthalpic and entropic factors contribute to the energy difference.

Our current investigation has provided an opportunity to manipulate enantiospecific photochemical transformations of axially chiral chromophores through H-bonding. The dynamic aspects that arise as a result of H-bonding offer new avenues to control and comprehend fundamental mechanistic features during light-induced transfer of molecular chirality.

■ ASSOCIATED CONTENT

Supporting Information. Experimental procedures, single-crystal XRD data (CIF), characterization data, and analysis conditions. This material is available free of charge via the Internet at http://pubs.acs.org.

■ AUTHOR INFORMATION

Corresponding Author
sivaguru.jayaraman@ndsu.edu

■ ACKNOWLEDGMENT

The authors thank the NSF for financial support (CAREER CHE-0748525) and generous funding through NSF-CRIF (CHE-0946990) for the purchase of departmental XRD instrumentation. Anoklase Ayitou, Barry Pemberton, and Ramya Raghunathan are thanked for help with manuscript preparation.

■ REFERENCES

(1) Doyle, A. G.; Jacobsen, E. N. *Chem. Rev.* **2007**, *107*, 5713.
(2) Inoue, Y. *Chem. Rev.* **1992**, *92*, 741.
(3) Sivaguru, J.; Natarajan, A.; Kaanumalle, L. S.; Shailaja, J.; Uppili, S.; Joy, A.; Ramamurthy, V. *Acc. Chem. Res.* **2003**, *36*, 509.
(4) Eliel, E. L.; Wilen, S. H. *Stereochemistry of Organic Compounds*; Wiley: New York, 1994; Chapter 14, pp 1119−1190.
(5) Curran, D. P.; Qi, H.; Geib, S. J.; DeMello, N. C. *J. Am. Chem. Soc.* **1994**, *116*, 3131.
(6) (a) Ayitou, A. J.-L.; Sivaguru, J. *J. Am. Chem. Soc.* **2009**, *131*, 5036. (b) Ayitou, A. J.-L.; Jesuraj, J. L.; Barooah, N.; Ugrinov, A.; Sivaguru, J. *J. Am. Chem. Soc.* **2009**, *131*, 11314. (c) Jesuraj, J. L.; Sivaguru, J. *Chem. Commun.* **2010**, *46*, 4791. (d) Ayitou, A. J.-L.; Sivaguru, J. *Chem. Commun.* **2011**, *47*, 2568.
(7) (a) Taylor, E. C.; Kan, R. O.; Paudler, W. W. *J. Am. Chem. Soc.* **1961**, *83*, 4484. (b) Ayer, W. A.; Hayatsu, R.; de Mayo, P.; Reid, S. T.; Stothers, J. B. *Tetrahedron Lett.* **1961**, *2*, 648. (c) Bach, T.; Bergmann, H.; Harms, K. *Org. Lett.* **2001**, *3*, 601. (d) Tanaka, K.; Fujiwara, T.; Urbanczyk-Lipkowska, Z. *Org. Lett.* **2002**, *4*, 3255.
(8) Garcia-Garibay, M. A.; Scheffer, J. R.; Watson, D. G. *J. Org. Chem.* **1992**, *57*, 241.
(9) The turn from the highest priority ligand in front of the chiral axis to the highest priority ligand behind the chiral axis is clockwise in the *P* configuration and counterclockwise in the *M* configuration.
(10) See the Supporting Information.
(11) Anslyn, E. V.; Dougherty, D. A. *Modern Physical Organic Chemistry*; University Science Books: Sausalito, CA, 2006; pp 145−205.
(12) Gilli, G.; Bertolasi, V.; Ferretti, V.; Gilli, P. *Acta Crystallogr.* **1993**, *B49*, 564.
(13) Hibbert, F.; Emsley, J. *Adv. Phys. Org. Chem.* **1991**, *26*, 255.
(14) Kitagawa, O.; Fujita, M.; Kohriyama, M.; Hasegawa, H.; Taguchi, T. *Tetrahedron Lett.* **2000**, *41*, 8539.
(15) (a) Matsumura, K.; Mori, T.; Inoue, Y. *J. Am. Chem. Soc.* **2009**, *131*, 17076. (b) Matsumura, K.; Mori, T.; Inoue, Y. *J. Org. Chem.* **2010**, *75*, 5461.